AIAA–2003–0183

Highly Inclined Jets in Cross Flow

I.M. Milanovic
University of Hartford
West Hartford, CT
and
K.B.M.Q. Zaman
NASA Glenn Research Center
Cleveland, OH

41st AIAA Aerospace Sciences Meeting and Exhibit
January 6–9, 2003 / Reno, Nevada

HIGHLY INCLINED JETS IN CROSS-FLOW

Ivana M. Milanovic*
University of Hartford
West Hartford, CT 06117

Khairul B. M. Q. Zaman†
NASA Glenn Research Center
Cleveland, OH 44135

Abstract

Results from an experimental investigation of flow field generated by pitched and yawed jets discharging from a flat plate into a cross-flow are presented. The circular jet was pitched at $\alpha = 20°$ and 45° and yawed between $\beta = 0°$ and 90° in increments of 15°. The measurements were performed with two ×-wires providing all three components of velocity and turbulent stresses. These data were obtained at downstream locations of x = 3, 5, 10 and 20, where the distance x, normalized by the jet diameter, is measured from the center of the orifice. Data for all configurations were acquired at a momentum-flux ratio J = 8. Additionally, for selected angles and locations, surveys were conducted for J = 1.5, 4, and 20. As expected, the jet penetration is found to be higher at larger α. With increasing β the jet spreads more. The rate of reduction of peak streamwise vorticity, ω_{xmax}, with the downstream distance is significantly less at higher β but is found to be practically independent of α. Thus, at the farthest measurement station x = 20, ω_{xmax} is about five times larger for $\beta = 75°$ compared to the levels at $\beta = 0°$. Streamwise velocity within the jet-vortex structure is found to depend on the parameter J. At J = 1.5 and 4, 'wake-like' velocity profiles are observed. In comparison, a 'jet-like' overshoot is present at higher J. Distributions of turbulent stresses for various cases are documented. Peak normal stresses are found to occur within the core of the streamwise vortices. With yaw, at lower values of J, high turbulence is also observed in the boundary layer underneath the jet-vortex structure.

Nomenclature

D	Nozzle diameter
J	Momentum-flux ratio, $J = (\rho_j U_j^2)/(\rho_\infty U_\infty^2)$
U	Mean jet or free-stream velocity normalized by U_∞
VR	Velocity ratio, $VR = U_j / U_\infty$
u, v, w	Mean velocity in streamwise, normal and spanwise direction normalized by U_∞
u', v', w'	Turbulence intensity in streamwise, normal and spanwise direction normalized by U_∞
$\overline{u'v'}$, $\overline{u'w'}$	Turbulent shear stresses normalized by U_∞^2
x, y, z	Cartesian coordinates normalized by D

Greek Symbols

α	Jet pitch angle relative to tunnel floor, degrees
β	Jet yaw angle relative to direction of cross-flow, degrees
ρ	Density
ω	Vorticity normalized by U_∞/D

Subscripts

j	Jet
max	Maximum
∞	Free stream

1. Introduction

Jets in cross-flow (JICF) have applications in a variety of technologically important systems and processes. In one form or another JICF is involved in active flow control, aircraft performance and stability, mixing augmentation, film and effusion cooling, etc. Before discussing the objectives of this study, we will review the flow features of JICF and some pertinent work from the literature. The presence of the high momentum transverse jet in a cross flow has the similar effect as that of a solid body. The retarded flow at the jet's 'leading' edge creates an increased pressure, while the 'trailing' edge is characterized by low pressure. The cross-flow deflects the jet into its characteristic trajectory and deforms the jet cross-section. At the same time, the cross flow shears the jet fluid around its perimeters, and the resulting vorticity distribution ultimately develops into a counter-rotating vortex pair. It has been shown that this streamwise vortex pair, which is the salient feature of a JICF, can persist for hundreds of diameters downstream.

---

* Member AIAA, Assistant Professor
† Associate Fellow AIAA, Aerospace Engineer

Investigation of the flow field of an inclined JICF dates back to the 1952, when Wallis[1] showed that a pitched and yawed jet produces a vortex system similar to one from a wing-type vortex-generator. Wu et al.[2] documented the flow topology of normal jets with different cross-sectional shape and $1 \le VR \le 9$ using flow visualization techniques. Note that for incompressible flow, the velocity ratio VR is the square root of the momentum-flux ratio J. In Ref. 2, comparisons of flow fields were made in an attempt to identify conditions that enhance asymmetry. Johnston and Nishi[3] studied jets pitched at 45° and yawed at 90° and 180° over a range of velocity ratios, $0.4 \le VR \le 1$. The emphasis was on the investigation of potential active flow control methods as an alternative to existing solid vortex generators. Lin et al.[4] examined 45° pitched jets at $1.7 \le VR \le 6.8$, as part of a comparative study on passive and active methods for flow control. Compton and Johnston[5] investigated the development of the mean velocity field from a single jet at 45° pitch, and at yaw angles up to 180°. Velocity ratios were varied from 0.7 to 1.3. The study indicated that an optimal yaw angle producing maximum vorticity might be between 45 and 90 degrees. Honami et al.[6] carried out a study of a jet at $\alpha = 30°$, $\beta = 90°$, and $0.5 \le VR \le 1.2$, for film cooling purposes. An increase in velocity ratio was shown to enhance asymmetry of the vortical system and reduce film-cooling effectiveness.

While the aforementioned investigations focused on the mean flow features, Zhang[7] carried out LDA measurements for pitch and yaw angles of 45° at velocity ratios up to 1.5, and also provided data on the turbulent stress field. Johnston and Khan[8-10] performed flow visualization as well as LDV measurements at α = 30° and 45°, β = 45°-90°, and $1 \le VR \le 1.5$. Quantitative information on the flow field included both mean and turbulent flow features. It was found that for a velocity ratio of 1, 30° pitch and 60° yaw produced the vortex with the peak mean vorticity. Jonhston[11] reviewed experimental and computational results on pitched and yawed JICF. The velocity ratio was found to be the principal design parameter if other parameters were kept within moderate limits. Bray[12] performed detailed five-hole probe surveys examining effects of pitch angle, yaw angle, diameter and Mach number ratio, as well as streamwise distance. In his low speed study, VR ranged from 0.7 to 2, and pitch and yaw angles were set to 30, 45 and 60 degrees. Comparisons between vane and air-jet vortices were also made. Bray and Garry[13] presented a correlation for maximum vorticity of a pitched and yawed JICF.

It is obvious that a lot of work has been done in the subject area. Yet, it should also be clear that because of the vast parameter space, a coherent understanding has not been achieved. Many aspects of the flow field such as the structure, trajectory and evolution of the streamwise vortices as a function of pitch and yaw angles and momentum-flux ratio, remain far from completely clear. Moreover, the literature lacks detailed measurements at low pitch, enhanced angular resolution in yaw, and high momentum-flux ratios. Such information is increasingly in demand by the designer of propulsion components. This provided the motivation for revisiting the subject and carrying out the present study. The objective was to obtain detailed quantitative data on the flow field evolution for systematic variation of certain parameters, as elaborated in the following. The experimental conditions and parametric ranges are described in the next section.

2. Experimental Setup

The investigation was conducted in a NASA GRC open circuit low-speed wind tunnel with 0.76 m × 0.51 m test section. The jet was produced with an inclined nozzle of diameter D = 19.05 mm. The nozzle was a straight hole cut through a clear plastic disc, of 25.4 mm thickness. The disc was mounted flush on the test section floor. Two discs were used to provide two pitch angles, (α = 20° and 45°), measured between the nozzle centerline and the floor of the test section. Each disk could be rotated to vary the yaw angle, β, measured between the nozzle centerline and the direction of the cross flow. The jet was yawed in 15° increments between 0° and 90°. A flow-conditioning screen was placed at the nozzle inlet, which was connected to compressed air supply through a flexible hose. An orifice meter fitted to the supply line was used to monitor the mass flow. The mass flow was used to calculate the mean jet velocity, U_j. All data were acquired for a constant free stream velocity of U_∞ = 8 m/s. The Reynolds number, based on free stream conditions and nozzle diameter was 9800.

The measurements were performed using hot-wire anemometry. Two ×-wires of different orientations could be traversed under automated computer control. The probes were stepped through the same grid points allowing the measurement of all three components of mean velocity and turbulence intensity. The origin of the coordinate is located at the center of the jet orifice. The streamwise (i.e., the cross-flow) direction is denoted by x, the direction normal to the tunnel floor is denoted by y, and the spanwise direction along the tunnel floor by z. At the downstream locations of 3, 5, 10 and 20 jet diameters from the orifice, the turbulent boundary layer had thicknesses of 0.60, 0.64, 0.684 and 0.822 jet diameters, respectively. The data for all configurations were acquired at a momentum-flux ratio

of 8. Additionally, for selected arrangements (α = 20° and 45°, β = 75°, x = 10) the momentum-flux ratio was set at 1.5, 4, and 20. The test-matrix involved a total of 48 cross-sectional surveys.

3. Mean Velocities

Contours of streamwise velocity distribution, u, for both pitch angles and zero yaw at momentum-flux ratio of 8, presented in Fig. 1, indicate symmetrical distribution around the z = 0 plane. Cross-flow vectors (v, w) show strong lateral flow towards the symmetry plane. As the fluid passage is restricted by the wall and the symmetry condition, flow is forced upward deforming the jet into a kidney shape. For a given downstream location, the upward penetration of the jet and the curvature of the jet cross-section are more pronounced at the higher pitch angle. An inspection of the contours indicate that the shape of the velocity profile in the plane of symmetry changes as follows. Velocity profiles at 20° pitch exhibit one peak. With increasing x, its magnitude decreases and the profiles become 'flatter'. The location of the peak shifts upwards. Velocity profiles at 45° pitch, on the other hand, indicate two peaks at measurement planes close to the orifice. However, further downstream the profiles are characterized by just one maximum value. Note that a similar dual-peak profile was observed by Sherif and Pletcher.[14] The present results also show that the 20° pitch case, compared to 45° case, is characterized by larger velocity magnitudes occurring closer to the wall.

Only key results for the pitched and yawed cases are presented. However, the discussion will draw on the entire dataset and comparison will be made with data from the literature wherever possible. Streamwise velocity contours for two representative yawed cases (α = 20° and 45°, β = 75° and $J = 8$) are shown in Fig. 2, capturing the evolution of the jet cross-section with increasing downstream distance. A comparison with corresponding data at zero yaw angle indicates that the yawed jet has spread much more.

In Fig. 3, the influence of momentum-flux ratio, for a given pitch and yaw, is examined at a fixed downstream location (x = 10). It can be seen that the jet-vortex fields at values of J greater than about 4 are characterized by velocities higher than U_∞. On the other hand, velocity deficits are observed at low momentum-flux ratios, as seen in the works of Compton and Johnston[5], Khan and Johnston[9-10], and Lee et al.[15] for J = 1. Gopalan et al.[16] also observed a fundamental change in the flow structure across a comparable threshold in J. The present results not only confirm the velocity deficit at low J, but also capture a systematic trend. Velocity overshoot becomes the prominent feature at higher momentum-flux ratios. Note that at intermediate values of J both deficit and overshoot take place within the jet-vortex structure. The present results, obtained up to x = 20, moreover indicate that the velocity deficit trend can persist farther downstream than previously found.

As observed in Fig. 2, increasing yaw angle introduces asymmetry in the velocity distributions. The location of the maximum velocity shifts away from the tunnel centerline with increasing downstream distance. A distorted kidney shape is initially discernible, with peak streamwise velocity located in a region closer to the centerline. In comparison to the zero yaw case, maximum velocities for β = 75° are closer to the wall and have considerably lower values. The kidney shape changes its orientation from 'horizontal' to 'vertical', and at the last measurement station, for α = 20°, only one local maximum is detected. Overall, the flow field for α = 45° and β = 75° indicates a similar behavior of outward translation and simultaneous counterclockwise rotation with downstream distance. Two distinct regions of velocity peaks are present and persist even at the last measurement location. The magnitudes of the peak streamwise velocity for four representative cases are shown in Fig. 4, as a function of x. It can be seen that a higher yaw angle results in considerably lower magnitudes at all measurement stations.

The jet was yawed in 15° increments between 0° and 90°, and data were collected for x = 3 and 10. Figure 5 shows the maximum velocity as a function of the yaw angle. It can be seen that the peak velocity decreases with increasing yaw angle. For both pitch angles this trend is non-linear at x = 3 but becomes almost linear at x = 10. As expected, the detailed data show that the location of u_{max} shifts upwards with the higher pitch, and outwards with higher yaw.

Recall that at low J, the jet-vortex is characterized by velocity deficit. This is examined further in Fig. 6 with velocity profiles through the point of minimum u, for x = 10 and J = 1.5 for selected angles. At zero yaw, velocity profiles for both pitch values exhibit one local minimum and one local maximum. The magnitude of the minima for both pitch are comparable and about $u \approx 0.85$, the one at higher pitch occurring farther away from the wall. The profiles for the 75° yaw case have one pronounced minimum, 0.69 for 20° pitch, and 0.79 for 45° pitch. These minima coincide with the core of the stronger vortex. At this high yaw angle, the weaker vortex has already been diffused. The deficit values compare well with the measurements of Khan and Johnston.[9-10] A configuration with α = 30° and β = 60° in Ref. 10, exhibited velocity minima of 0.7 and 0.85, at x = 10, for J = 1 and 2.25, respectively.

4. Mean Streamwise Vorticity

Contours of streamwise vorticity distribution, ω_x, for the configurations of Fig. 2, are presented in Figure 7. In the case of zero yaw, the counter-rotating vortex pair moves away from the wall and apart from each other with the downstream distance. For increased yaw, the vortex with the positive vorticity becomes the dominant structure. Its strength at the downstream locations is as large as six times that of the weaker vortex. There is also a net transport of the vortex system laterally in the yawed direction. The dominant vortex facilitates a movement of low momentum flow close to the wall into the weak vortex. At the upstream locations additional concentrations of negative vorticity are observed near the wall, presumably due to reorientation of the boundary layer. Merger of structures with negative vorticity is achieved faster for the lower pitch angle due to their proximity to each other. The region of concentrated negative vorticity is then quickly diffused and dissipated further downstream. At the last measurement station, essentially a single vortex with the positive vorticity remains.

It may be observed in Fig. 7 that the peak streamwise vorticity, ω_{xmax}, decreases with the downstream distance. This trend is clearly shown in Fig. 8 for both pitch cases. At zero yaw, ω_{xmax} is found to become half of the initial value by x = 5, and by the last measurement station it is reduced to about one tenth. The rate of decrease for the β = 75° is more gradual and a vortex of considerable strength remains at x = 20. The magnitudes at different pitch angles but same yaw compare closely, however, as already stated, the rate of decrease is much lower at the higher yaw case. This finding reveals that if an application requires longer persistence of streamwise vorticity, yawed jets are advantageous. The result also appears to be characteristic of a range of J investigated in the present experiments, as clearly evident from the data shown in Fig. 9. The changes in ω_{xmax} are small for all cases when the momentum-flux ratio is increased beyond a value of about four.

Referring back to Fig. 7, the streamwise vorticity is examined further. At the first measurement station and 20° pitch, the vortex pair changes its structure with an increase in yaw. For β = 60° and higher, the flow field seems to result in two regions of loosely dispersed positive vorticity instead of a single concentrated vortex (x = 3, 5; Fig. 7). Such an occurrence is also observed in Ref. 9 for the case of J = 1, α = 30°, and β = 60°. Obviously, the flow is in an early stage of the rolling up process at the upstream location. For both pitch angles, at x = 10, well-defined concentrated vorticity is ultimately developed as the flow field is allowed the necessary distance to evolve.

The variation of peak streamwise vorticity as a function of yaw angle for the positive vortex is summarized in Fig. 10 for J = 8, at x = 3 and 10. For all cases the trends are non-linear. At x = 3, maximum streamwise vorticity for 20 and 45 degree pitch is achieved respectively at 15° and 30° yaw. At x = 10, peak vorticity values for α = 20° and 45° are found at β = 60° and 45°, respectively.

In an attempt to assess the relative influence of the high momentum versus high vorticity regions of the flow on boundary layer separation, streamwise velocity gradients were compared at the x-locations of u_{max} and ω_{xmax} (data not shown). Cases considered included all measurement stations for J = 8 and all momentum-flux ratios at x = 10, for α = 20° and 45° and β = 75°. Using $\partial u/\partial y$ near the wall as the first order indicator, the trends suggested that the proximity of the high vorticity portion of the jet-vortex rather than the high momentum portion might be somewhat more effective in prevention of boundary layer separation.

5. Turbulent Stresses

Contour plots of turbulent normal stresses are presented for the same combinations of parameters as considered in the previous sections. The distributions of u', v' and w' at J = 8, α = 20° and β = 75°, are shown in Figs. 11-13. Maximum magnitudes for all three stresses decrease with increasing downstream distance. The peak value of u' is larger than those of v' and w' at the upstream measurement locations but at x = 20 the levels have become comparable. Corresponding data for zero yaw (not shown) indicate that the turbulent structure changes its shape and spreads with increasing x, commensurate with the U-distributions. The smaller pitch angle produces overall larger peaks in u'.

Comparison of Figs. 11-13 with Fig. 7(a) makes it clear that the regions of peak turbulence correlate well with regions of peak ω_x. There are a few likely explanations for this. The core of a streamwise vortex entrains surrounding turbulence.[17] The core acts as a wave guide propagating disturbances that would have otherwise dissipated.[18] Vortex meandering could be significant factor in the appearance of high 'turbulence'.[9] The precise mechanism remains unclear, however, investigation of delta wing flow field[19] suggests that ingestion or entrainment of turbulence from surrounding flow may be the primary reason. The levels of peak turbulence intensities are in agreement with previous findings of Zhang[7] and Khan and Johnston.[9]

Characteristic u'-distributions for varying J are shown in Fig. 14. Maximum turbulence intensity increases with increasing J. For J = 1.5 the vortex is in the proximity of the tunnel wall, and u'_{max} region encompasses the vortex core and the boundary layer beneath it. For J greater than 1.5, region of maximum turbulence coincides with the core, while significant levels are still found beneath the vortex. As the vortex moves upward with increasing J, the boundary layer immediately below the core is affected less. There might be an optimal J, for the given pitch and yaw, at which the boundary layer is 'energized' the most.

The measurements also included two shear stress components, $\overline{u'v'}$ and $\overline{u'w'}$. The influence of momentum-flux ratio on $\overline{u'v'}$ is shown in Fig. 15 for 20° pitch and 0° and 75° yaw. At zero yaw the positive and negative $\overline{u'v'}$ run alongside and almost parallel to the wall, with relatively large magnitudes. For the yawed case, at low J, the flow field is characterized by regions of positive and negative $\overline{u'v'}$ located below and above the vortex core, respectively. Similar distributions and levels have been observed in the works of Zhang[7] and Khan and Johnston.[9] As with u' distributions, there exists significant $\overline{u'v'}$ levels below the jet-vortex region near the wall.

The downstream evolution of $\overline{u'w'}$ distribution at β = 0° and 75°, is given in Figs. 16 (a)-(b), respectively, for J = 8 and α = 20°. For zero yaw, stronger levels are observed but away from the boundary layer. For the yawed case, a concentrated positive $\overline{u'w'}$ region is found to sweep across the boundary layer with increase in downstream distance. Therefore, from all the turbulence quantities measured, the yawed case is found to be more effective in 'energizing' the boundary layer. Hence, the yawed jets should be more efficient in boundary layer separation control.

5. Concluding Remarks

An experimental investigation of pitched and yawed JICF was carried out. To complement the existing literature, this work provided data for the low pitch angle and high momentum-flux ratios, with enhanced angular resolution in yaw.

The results for both pitch angles reveal that yawed jets are advantageous for applications requiring longer persistence of peak streamwise vorticity. Maximum streamwise vorticity for 20 and 45 degree pitch at J = 8 and x = 3 is attained respectively at about 15 and 30 degree yaw. Peak vorticity values for the same $\alpha - J$ combinations farther downstream (x = 10), are found to shift to the higher yaw angles: 60° and 45°, respectively. In the range of momentum-flux ratios examined, both velocity deficit and overshoot in the jet-vortex structure are observed. The deficit occurs at lower J while overshoot is typical at higher J. An examination of the velocity gradients near the wall reveals that the proximity of the vortex portion of the jet-vortex system might be somewhat more effective in boundary layer separation control.

The spatial reorganization of turbulence quantities and change in turbulence levels with the angles and momentum-flux ratios are documented. The flow is generally anisotropic. Peak normal stresses are found to occur within the vortex core. It is conjectured that this is mainly due to ingestion of turbulence from the surrounding flow. For same yaw, the smaller pitch angle produces overall larger peaks in u', v' and w'. Highly yawed jets are found to remain closer to the wall and enhance turbulence in the vicinity of the boundary layer. This effect is most pronounced in a lower range of momentum-flux ratios.

Acknowledgements

The work was supported by NASA-OAI Collaborative Aerospace Research and Fellowship Program. The first author is grateful to Connecticut Space Grant College Consortium—EPSCoR Core Funding for providing support. The authors are also thankful to Dr. Bruce Wendt of NASA GRC and Dr. Frank Y. Wang of DOT/Volpe for the valuable discussions.

References

[1]Wallis, R. A., "The Use of Air Jets for Boundary Layer Control", Aerodynamics Research Laboratories, Australia, *Aero Note* 110, N–34736, 1952.

[2]Wu, J. M., Vakili, A. D., and Yu, F. M., "Investigation of the Interacting Flow of Nonsymmetric Jets in Crossflow", *AIAA Journal*, Vol. 26, No. 8, August 1988, pp. 940–947.

[3]Johnston, J. P. and Nishi, M., "Vortex Generator Jets – Means for Flow Separation Control", *AIAA Journal*, Vol. 28, No. 6, June 1990, pp. 989–994.

[4]Lin, J. C., Howard, F. G., and Selby, G. V., "Investigation of Several Passive and Active Methods for Turbulent Flow Separation Control", *AIAA Paper* No. 90-1598, AIAA 21st Fluid Dynamics, Plasma Dynamics and Lasers Conf., June 18–20, 1990.

[5]Compton, D. A. and Johnston, J. P., "Streamwise Vortex Production by Pitched and Skewed Jets in a Turbulent Boundary Layer", *AIAA Journal*, Vol. 30, No. 3, March 1992, pp. 640–647.

[6]Honami, S., Shizawa T. and Uchiyama A., "Behavior of the Laterally Injected Jet in Film Cooling: Measurements of Surface Temperature and Velocity/Temperature Field Within the Jet", *Journal of Turbomachinery,* Vol. 116, January 1994, pp. 106–112.

[7]Zhang, X., "Turbulence Measurements of a Longitudinal Vortex Generated by an Inclined Jet in a Turbulent Boundary Layer", *Journal of Fluids Engineering*, Vol. 120, December 1998, pp. 765–771.

[8]Johnston, J. P. and Khan, Z. "The Origins of the Dominant Vortex From a Pitched and Skewed Jet", *JSME International Conference on Fluids Engineering,* Tokyo, Japan, Vol. I, 1997, pp. 321–326.

[9]Khan, Z. U. and Johnston, J. P., "On Vortex Generating Jets", *International Journal of Heat and Fluid Flow*, Vol. 21, 2000, pp. 506–511.

[10]Johnston, J. P., Mosier, B. P. and Khan, Z. U., "Effects of Inlet Conditions on Skewed and Pitched Jets in Cross-Flow", *2nd International Symposium on Turbulent Shear Flow Phenomena*, Stockholm, June 2001, pp. 1–6.

[11]Johnston, J. P., "Pitched and Skewed Vortex Generator Jets for Control of Turbulent Boundary Layer Separation: A Review", FEDSM99–6917, Proceedings of the *3rd ASME/JSME Joint Fluids Engineering Conference*, July 1999, San Francisco, California, pp. 1–10.

[12]Bray, T. P., "A Parametric Study of Vane and Air-Jet Vortex Generators", Ph.D. Thesis, Cranfield University, College of Aeronautics, Flow Control & Prediction Group, October 1998.

[13]Bray, T. P. and Garry, K. P., "Optimization of Air-Jet Vortex Generators with Respect to System Design Parameters", *The Aeronautical Journal,* October 1999, pp. 475–479.

[14]Sherif, S. A., and Pletcher, R. H., "Measurements of the Flow and Turbulence Characteristics of Round Jets in Crossflow", *Journal of Fluids Engineering,* Vol. 111, June 1989, pp. 165–171.

[15]Lee, S. W., Lee, J. S., and Ro, S. T., "Experimental Study on the Flow Characteristics of the Streamwise Inclined Jets in Crossflow on Flat Plate", *International Gas Turbine and Aeroengine Congress and Exposition*, Cologne, Germany, June 1992, pp. 1–9.

[16]Gopalan, S., Abraham, B., and Katz, J., "Turbulent Jet Injected into a Cross Flow—Analysis of the Flow Structure and Wall Pressure Fluctuations", FEDSM2002–31420, *ASME Fluids Engineering Conference,* Montreal, Canada, July 14–18, 2002.

[17]Bandypadyay, P. R., Stead, D. J., and Ash, R. L., "Organized Nature of a Turbulent Trailing Vortex", *AIAA Journal*, Vol. 29, No. 10, October 1991, pp. 1627–1633.

[18]Leibovich, S., "Vortex Stability and Breakdown: Survey and Extension", *AIAA Journal*, Vol. 22, September 1984, pp. 1192–1206.

[19]Wang, F.Y., Milanovic, I.M., and Zaman, K.B.M.Q., "A Quantitative Comparison of Leading-Edge Vortices in Incompressible and Supersonic Flows", *AIAA Paper* 2002–0557, 40th AIAA Aerospace Sciences Meeting, Reno, NV, Jan., 2002.

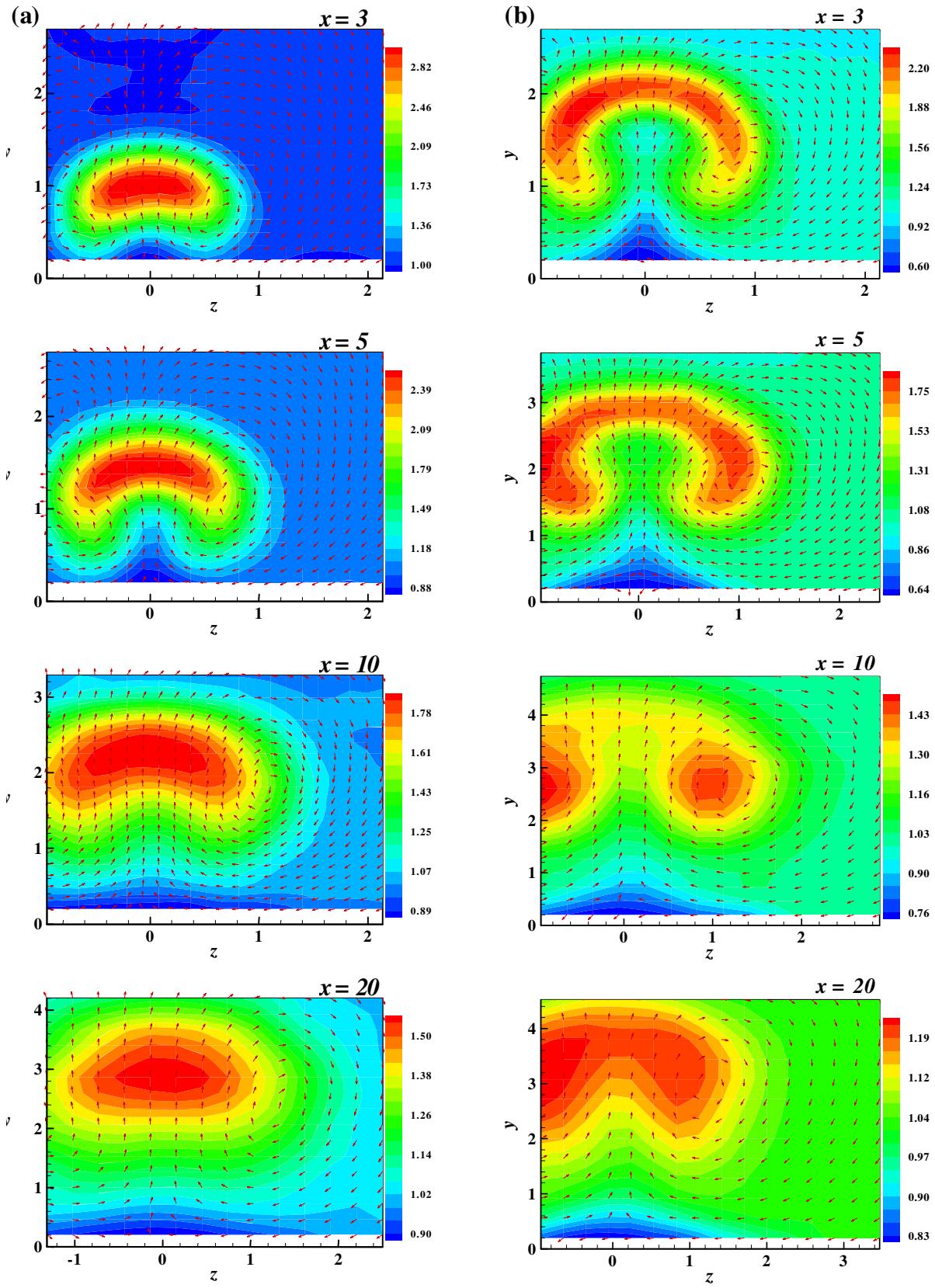

Fig. 1 Downstream evolution of streamwise velocity distribution; $\beta = 0°$, $J = 8$, (a) $\alpha = 20°$, (b) $\alpha = 45°$.

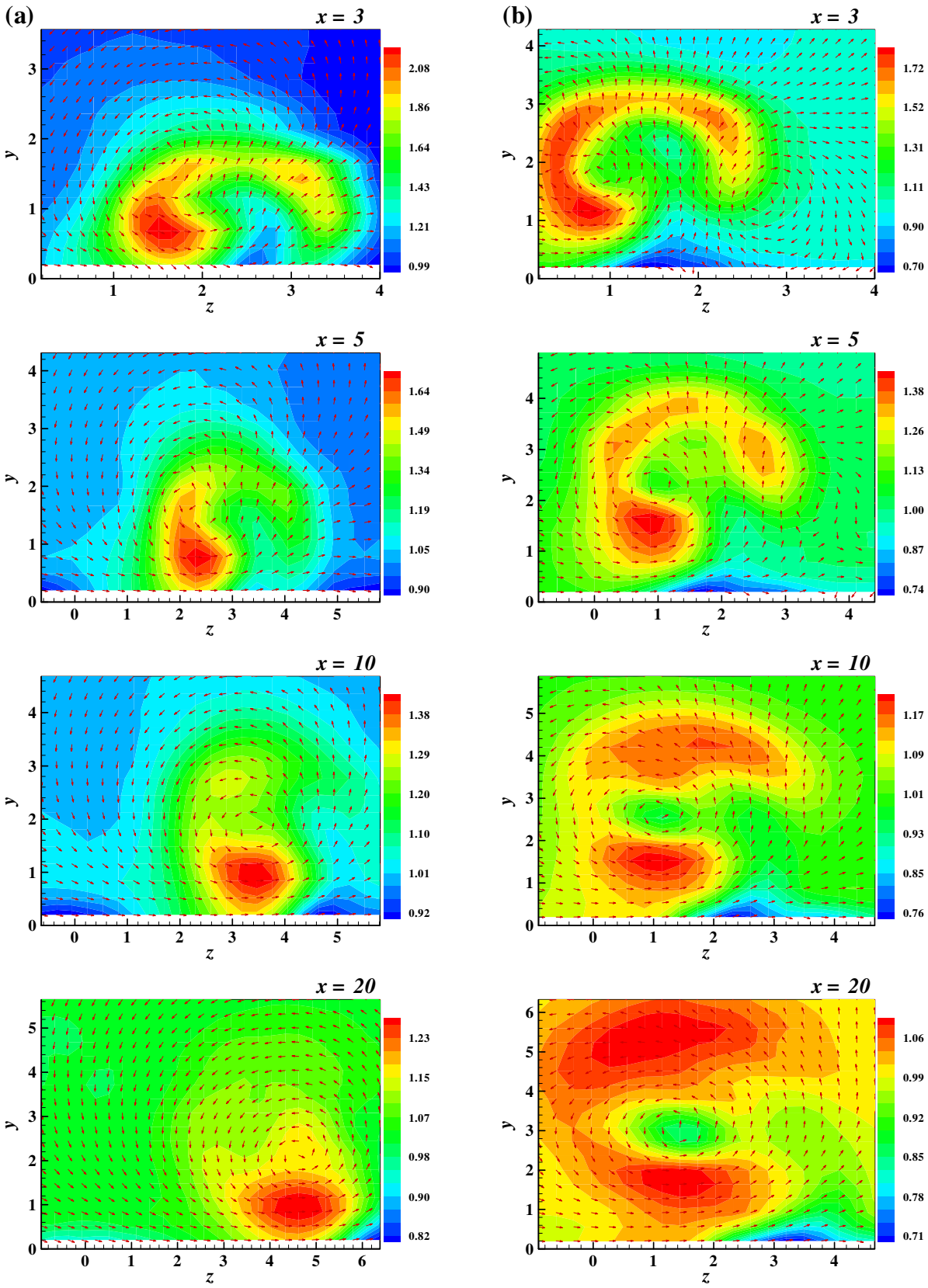

Fig. 2 Downstream evolution of streamwise velocity distribution; $\beta = 75°$, $J = 8$, (a) $\alpha = 20°$, (b) $\alpha = 45°$.

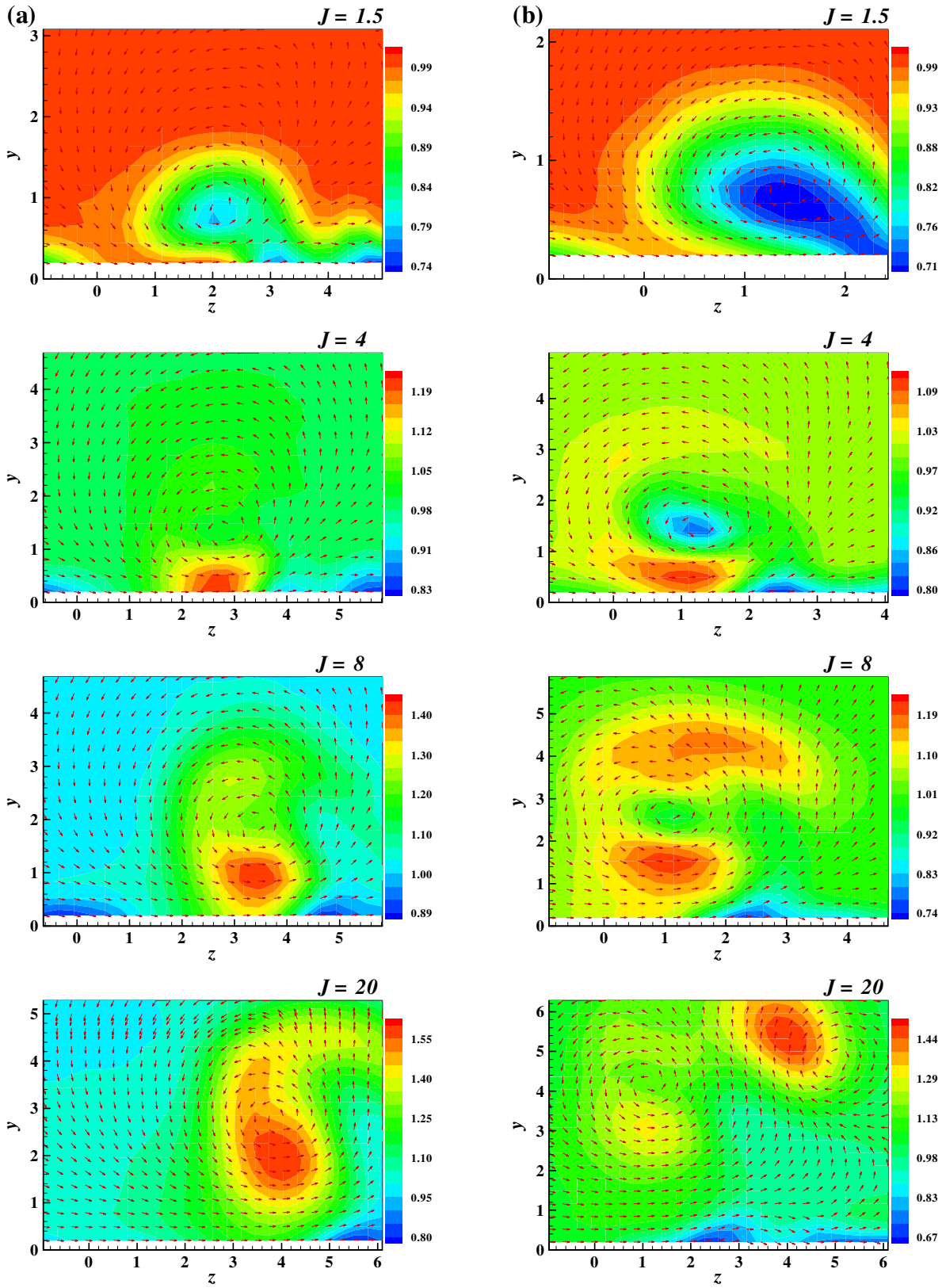

Fig. 3 Streamwise velocity distribution for various momentum-flux ratios; $\beta = 75°$, $x = 10$, (a) $\alpha = 20°$, (b) $\alpha = 45°$.

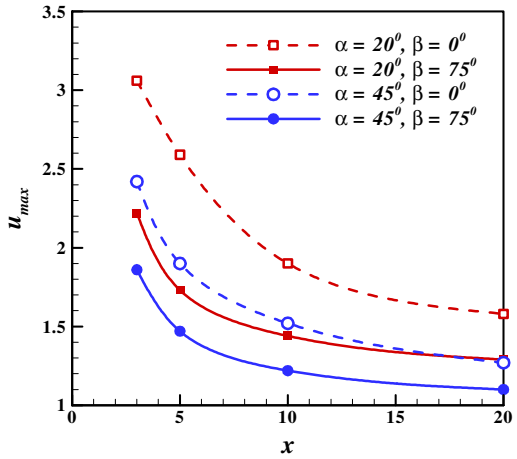

Fig. 4 Maximum streamwise velocities at various measurement planes; $J = 8$.

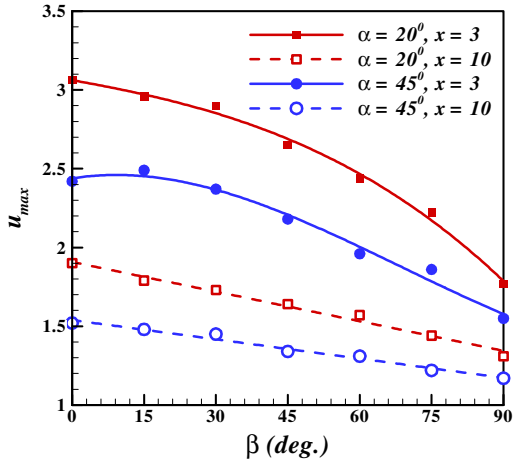

Fig. 5 Maximum streamwise velocities vs. yaw angle; $J = 8$.

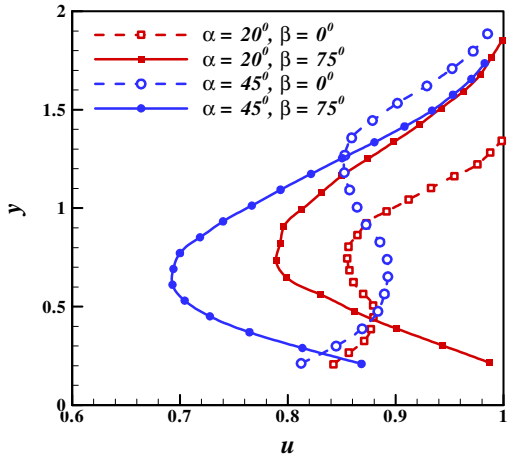

Fig. 6 Velocity profiles through the point of minimum velocity; $J = 8$, $x = 10$.

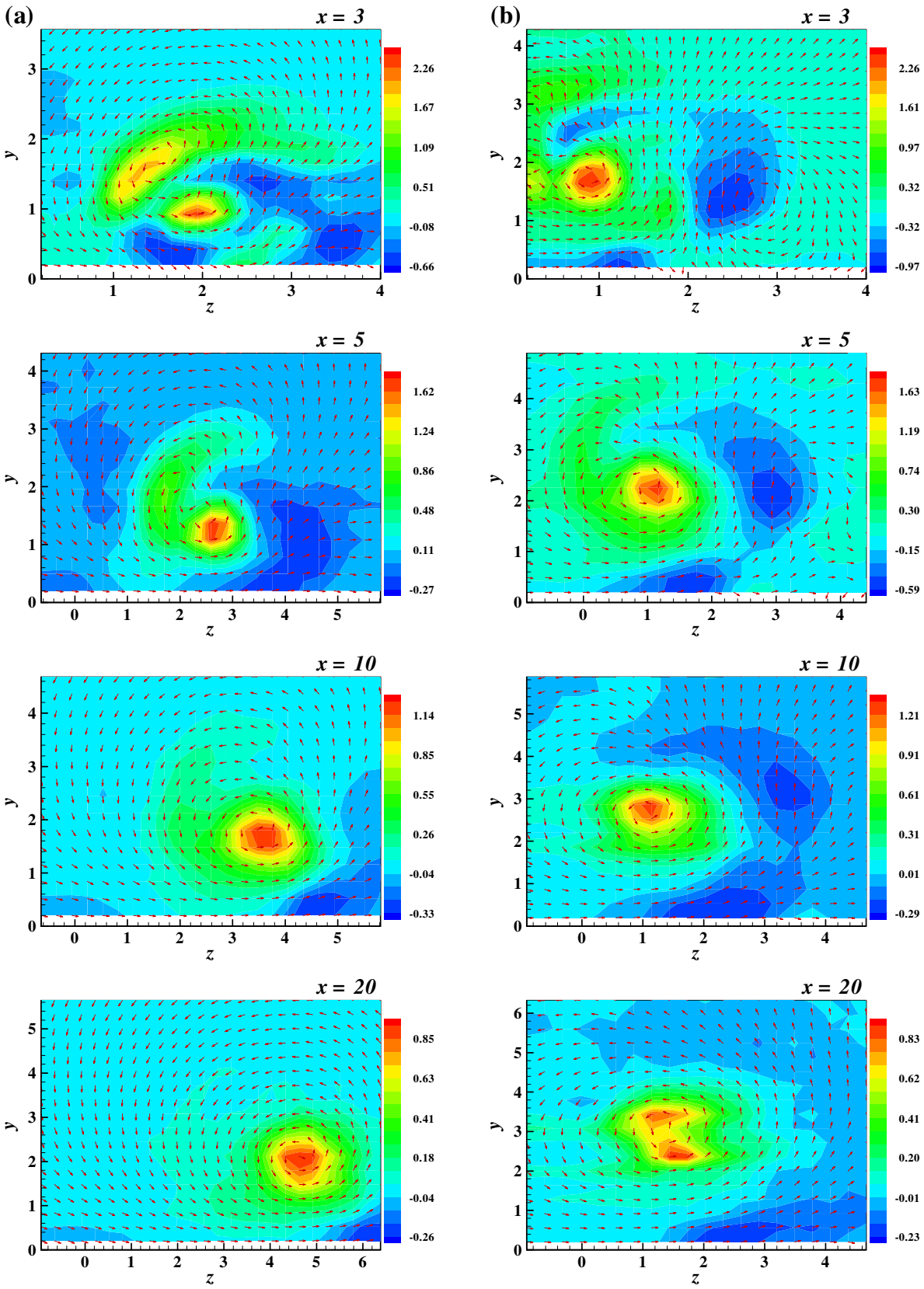

Fig. 7 Downstream evolution of streamwise vorticity distribution; $\beta = 75°$, $J = 8$, (a) $\alpha = 20°$, (b) $\alpha = 45°$.

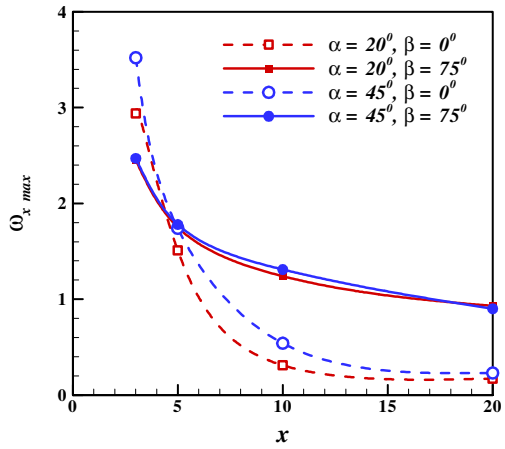

Fig. 8 Maximum streamwise vorticity as a function of downstream disance; $J = 8$.

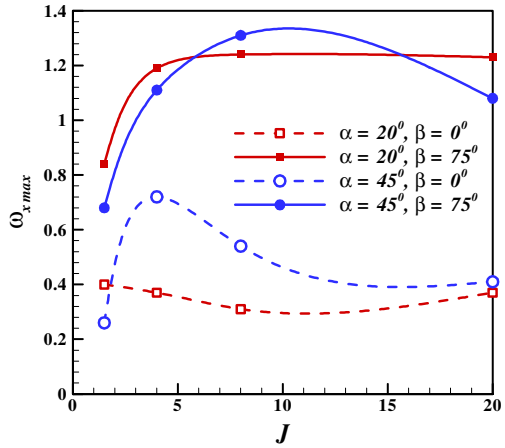

Fig. 9 Maximum streamwise vorticity as a function of momentum-flux ratio; $x = 10$.

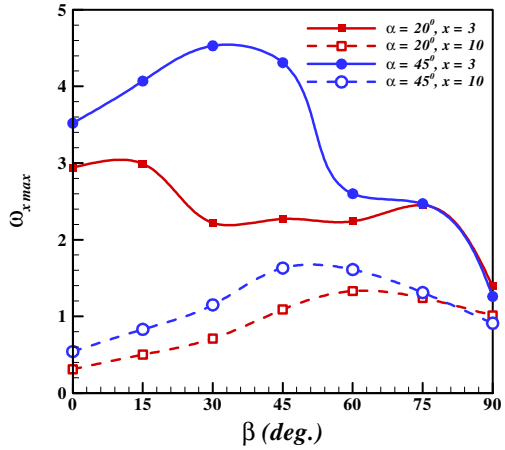

Fig. 10 Maximum streamwise vorticity as a function of yaw angle; $J = 8$.

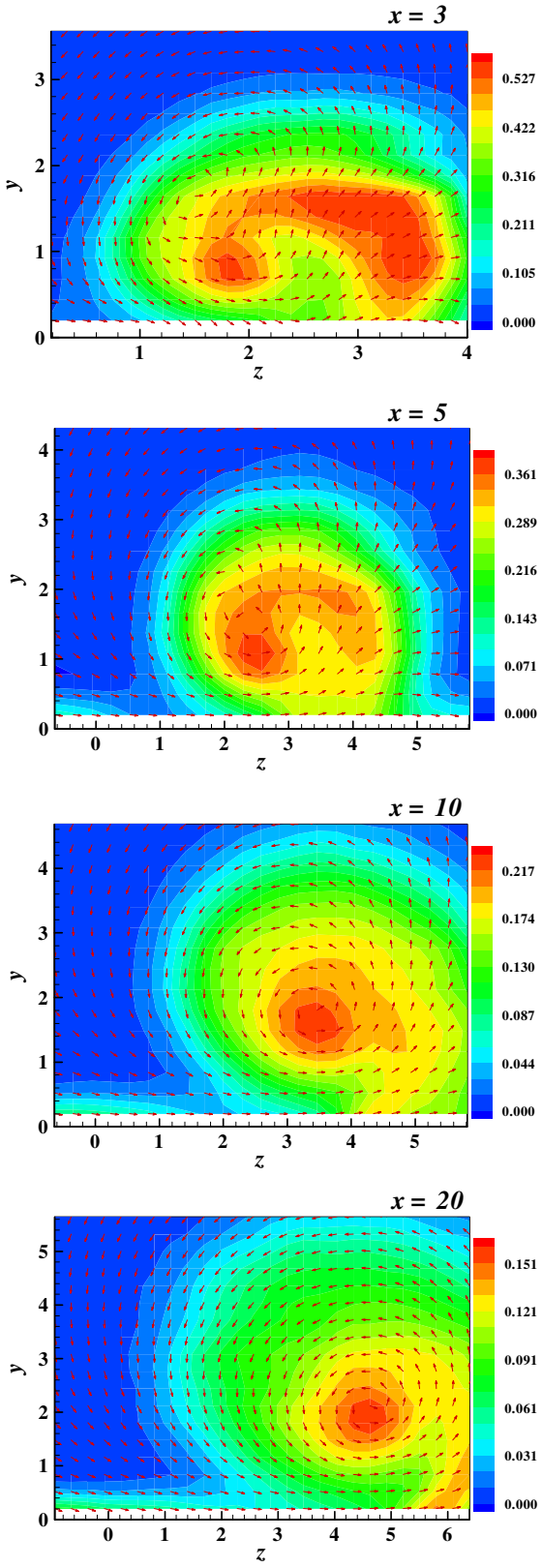

Fig. 11 Downstream evolution of streamwise turbulence intensity distribution; $\alpha = 20°$, $\beta = 75°$, $J = 8$.

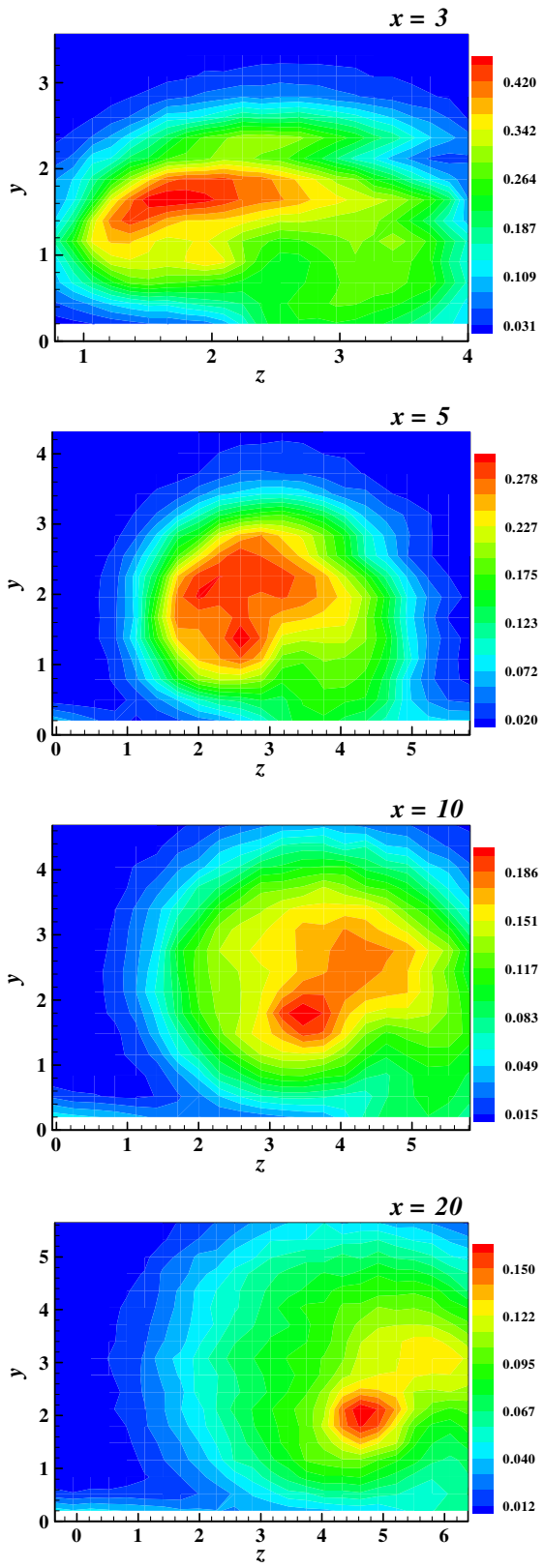

Fig. 12 Downstream evolution of normal turbulence intensitydistribution; $\alpha = 20°$, $\beta = 75°$, $J = 8$.

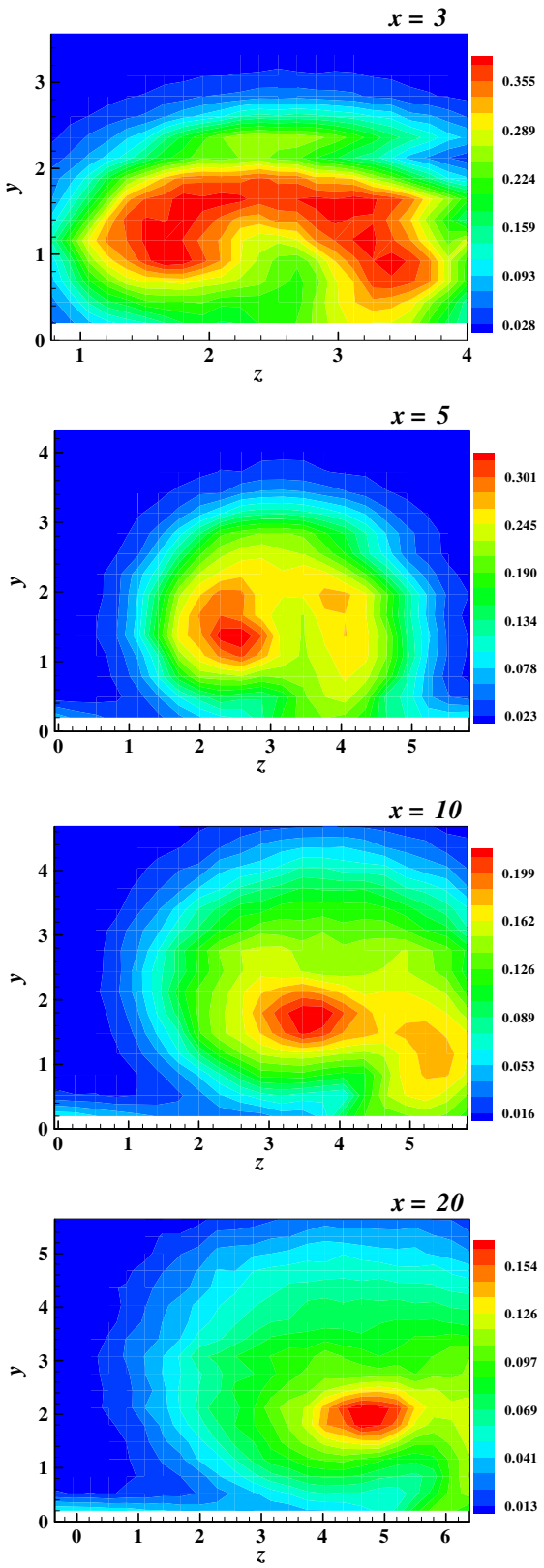

Fig. 13 Downstream evolution of spanwise turbulence intensity distribution; $\alpha = 20°$, $\beta = 75°$, $J = 8$.

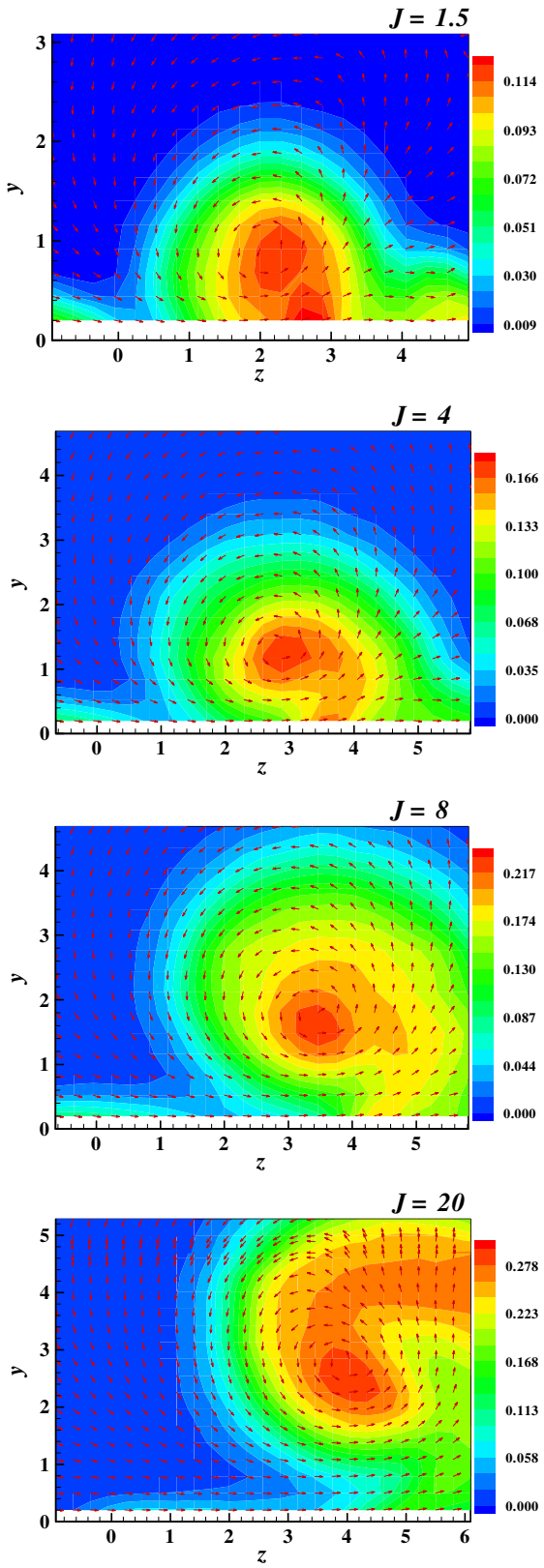

Fig. 14 Streamwise turbulence intensity distribution for various momentum-flux ratios; $\alpha = 20°$, $\beta = 75°$, $J = 8$.

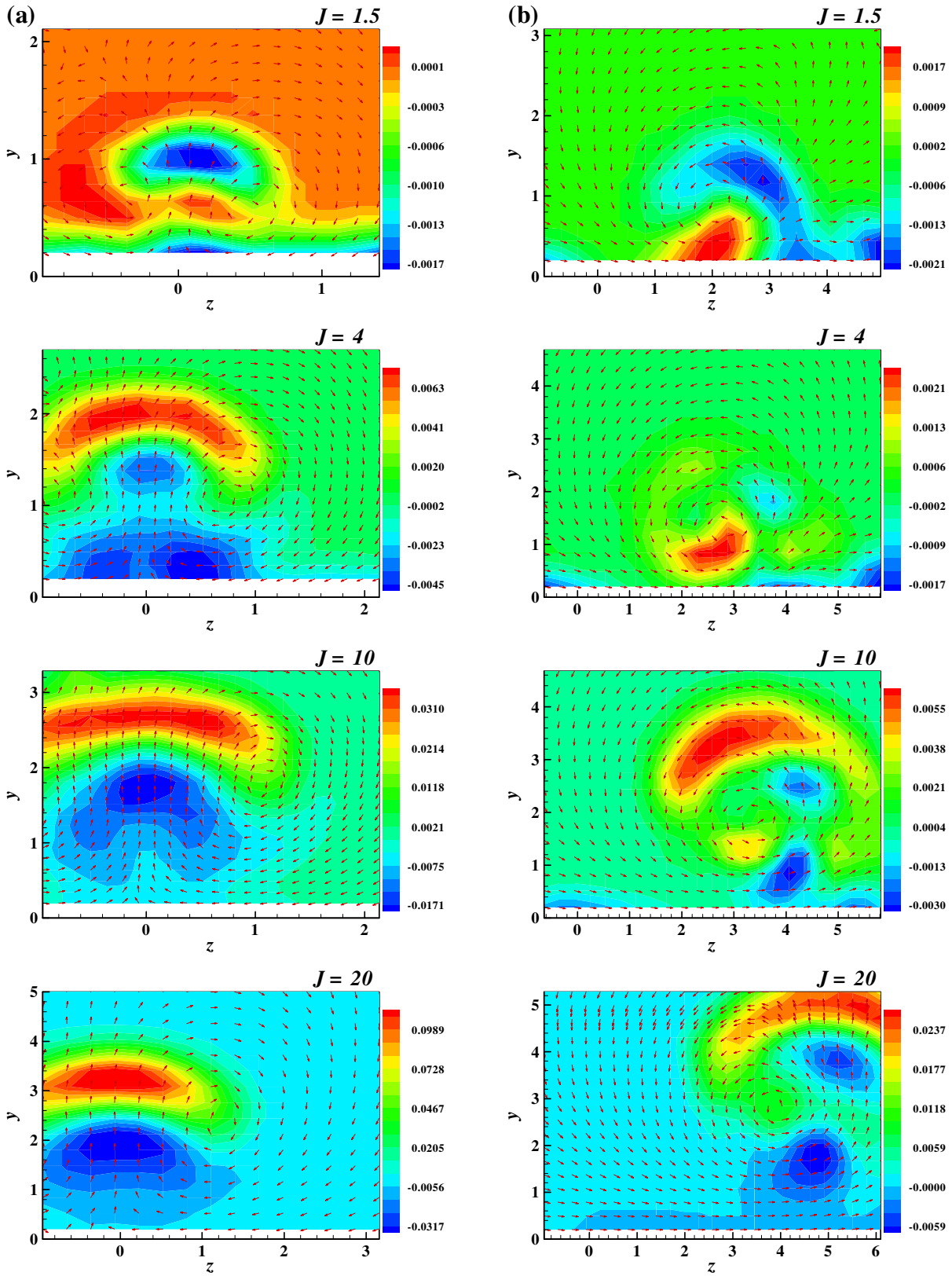

Fig. 15 Contours of $\overline{u'v'}$ for various momentum-flux ratios; $\alpha = 20°$, $x = 10$, (a) $\beta = 0°$, (b) $\beta = 75°$.

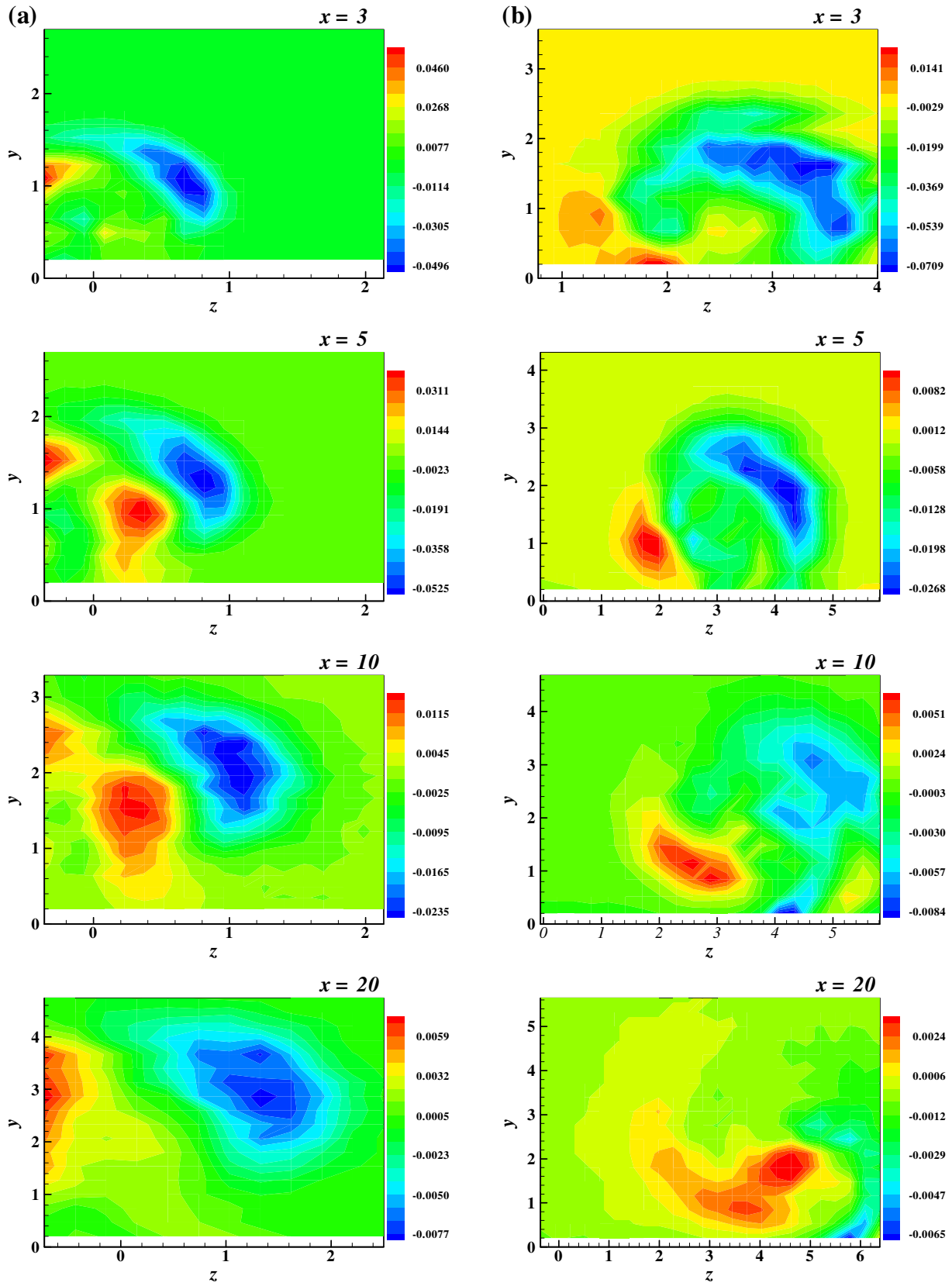

Fig. 16 Downstream evolution of $\overline{u'w'}$ distribution; $\alpha = 20°$, $J = 8$, (a) $\beta = 0°$, (b) $\beta = 75°$.